Original Article Open Access





DOI: 10.32768/abc.7581039462-817

Growth Inhibitory Effects of a Chinese Nutritional yedoensis, in a Model for Triple-Negative Breast Cancer

Nitin T. Telang*a Hareesh B Nair George Y-C Wongc,d

^aCancer Prevention Research Program, Palindrome Liaisons Consultants, Montvale, New Jersey, USA

^bUniversity of Texas Health Sciences Center, San Antonio, Texas, USA

^cAmerican Foundation for Chinese Medicine, New York, New York, USA

^dBreast Center Maimonides Medical Center, Brooklyn, New York, USA

ARTICLE INFO

ABSTRACT

Received: 28 May 2025 Revised: 20 August 2025 Accepted: 23 August 2025

Background: The triple-negative breast cancer (TNBC) subtype lacks the expression of hormone and growth factor receptors. Therapeutic options for TNBC include conventional cytotoxic chemotherapy and pathway-selective targeted therapy. These options are associated with therapy resistance and the emergence of cancer stem cells, leading to metastatic disease progression. Nontoxic nutritional herbs used in traditional Chinese medicine (TCM) may represent testable therapeutic alternatives. This study aimed to examine the growth-inhibitory efficacy of the nutritional herb Viola vedoensis (VY) and identify its mechanism of action in the MDA-MB-231 model of TNBC.

Methods: The effects of VY on cell proliferation, retinoblastoma (RB) signaling, and apoptosis were determined to examine its antiproliferative and proapoptotic efficacy.

Results: Treatment with VY resulted in S-phase arrest and inhibition of the RB signaling pathway by reducing cyclin E, CDK2, pRB, and E2F1 expression. The induction of apoptosis increased the sub-G0/G1 phase apoptotic population and increased proapoptotic caspase 3/7 activity. The VY-induced increase in caspase 3/7 activity was inhibited by a pan-caspase inhibitor.

Conclusion: These data identify the growth-inhibitory mechanism of VY, thereby providing a validated experimental approach to identify nutritional herbs as potential therapeutic alternatives for breast cancer.

Copyright © 2025. This is an open-access article distributed under the terms of the Creative Commons Attribution-Non-Commercial 4.0 International License, which permits copy and redistribution of the material in any medium or format or adapt, remix, transform, and build upon the material for any purpose, except for commercial purposes

Keywords: Viola yedoensis, retinoblastoma, triple-

negative breast cancer

INTRODUCTION

The clinical triple-negative breast cancer (TNBC) subtype lacks the expression of hormone and growth factor receptors, represents 15% to 20% of all cases of breast cancer, and is notable for an ethnic disparity favoring the African American population.¹ The TNBC subtypes exhibit pronounced heterogeneity that predisposes to cellular plasticity and phenotypic

*Address for correspondence:

Nitin T. Telang, Ph.D.,

Cancer Prevention Research Program, Palindrome Liaisons Consultants, 10 Rolling Ridge Road, Suite B, Montvale, New Jersey, USA

Email: ntelang3@gmail.com

diversity, leading to aggressive metastatic cancer progression.²

The lack of hormone and growth factor expression necessitates the use of conventional chemotherapy, including anthracycline-, platinum-, and taxane-based chemotherapeutics. However, longterm use of these pharmacological agents leads to systemic toxicity, acquired therapy resistance, and survival of a chemoresistant, cancer-initiating stem population.^{3,4} These clinical limitations emphasize the need for the identification of effective, nontoxic, testable alternatives.



Nutritional herbs constitute important components of herbal formulations that are widely used in traditional Chinese medicine (TCM). Chinese nutritional herbs have a long history of human consumption, a low degree of systemic toxicity, and mechanistic leads for preclinical efficacy. These aspects provide a rationale for investigating the growth-inhibitory efficacy of Chinese nutritional herbs as testable alternatives for breast cancer.

Published evidence on the MDA-MB-231 model for TNBC has demonstrated the antiproliferative and proapoptotic effects of several nutritional herbs, such as Dipsacus asperoides (DA), Cornus officinalis Psoralea corylifolia (PC). (CO), and antiproliferative effects have been associated with the inhibition of retinoblastoma (RB), RAS oncogene, phosphoinositide 3-kinase (PI3K), and protein kinase B (AKT) signaling pathways. The proapoptotic effects have been associated with the upregulation of caspases and modulated expression of apoptosisspecific proteins.5-9 The RAS, PI3K, and AKT signaling pathways are commonly activated in proliferating cancer cells and provide a growth advantage to primary cancer, as well as to therapyresistant cancer stem cells. 10

The Chinese nutritional herb *Viola yedoensis* (VY) is a common constituent in herbal formulations used in TCM. VY has documented efficacy as an antioxidant, antipyretic, and anti-inflammatory agent. ¹¹ Published evidence has also suggested that at a mechanistic level, VY functions as a potent inhibitor of the induced nitric oxide synthase (iNOS), cyclooxygenase-2 (COX-2), and nuclear factor-κB (NF-κB) pathways. ¹²

In the Lewis lung carcinoma model, VY functions as an anti-invasive agent affecting matrix metalloproteinase and urokinase-type plasminogen activator. ¹³ However, the anticancer activity of VY in breast cancer subtypes has not been unequivocally established. The lack of sufficient information about the growth-inhibitory efficacy of VY in breast cancer provides the rationale for the present study. Experiments in this study were designed to examine the growth-inhibitory effects of VY in a cellular model for TNBC and to identify effective mechanistic pathways and potential molecular targets.

METHODS

Experimental model

The MDA-MB-231 cellular model was established from the pleural effusion of a patient with metastatic breast cancer. These cells lack the expression of receptors for estrogen, progesterone, and human epidermal growth factor and represent a model for clinical TNBC.¹⁴ The MDA-MB-231 cell

line was obtained from the American Type Culture Collection (ATCC, Manassas, VA, USA), and was maintained in RPMI medium with L-glutamine and supplemented with 5% fetal bovine serum (Life Technologies, Grand Island, NY, USA). The cultures were routinely expanded at a 1:4 ratio when 70% confluent.

Test agent

The Chinese nutritional herb VY is a common constituent in herbal formulations used in TCM. This herb was provided by Dr. George YC Wong (coauthor). Traditionally, herbal formulations in TCM are prepared as an aqueous decoction in boiling water for patient consumption. To simulate this, a nonfractionated aqueous extract from the leaves of VY was prepared following an optimized, published protocol.⁵⁻⁹ The stock solution (aqueous supernatant) was obtained after multiple boiling and centrifugation cycles at a VY concentration of 20 mg/20 mL. This stock solution was reconstituted in the RPMI culture medium at a concentration of 1 mg/mL. For the experiments on cell cultures, the RPMI stock was serially diluted using the RPMI culture medium to obtain the final concentration range in µg/mL.

Dose response of VY

To determine the effective growth-inhibitory concentration range for VY, cell viability was monitored using the CellTiter-Glo assay (Promega Corporation). The cells were treated with VY at a concentration range of 20, 40, 80, 100, and 400 μg/mL for 6 days, and the cultures were maintained at 37 °C in a CO₂ incubator. Cells maintained without any treatment served as the control. Cell viability was measured using a Fluoroskan plate reader (Thermo Fisher Scientific Inc). The data were presented as relative luminescent units (RLUs) and as the percentage of inhibition relative to the untreated control.

Anchorage-independent growth assay

To perform the anchorage-independent (AI) growth assay, a suspension of MDA-MB-231 cells was prepared in 0.33% agar at a cellular density of 5.0 × 10⁵/mL. The cell suspension was treated with VY at concentrations of 100, 500, and 1000 μg/mL; cells without any treatment served as the untreated control. The cell suspensions were overlaid on a basement layer of 0.6% agar. The cultures were maintained at 37 °C in a CO₂ incubator for 21 days, and AI colonies formed in 0.33% agar were counted at ×10 magnification.⁸ The data were presented as the AI colony number and as the percentage of inhibition relative to the untreated control.

Cell cycle progression

For the cell cycle progression assay, cells were treated with VY at concentrations of 20, 40, and 80 μg/mL. Cells maintained in the culture medium without any treatment served as the control. Cell cycle analysis was performed according to an optimized and published protocol. The DNA content of cells was determined using a Becton Dickinson FACScan Flow Cytometer (BD Biosciences, Research Triangle Park, NC, USA) and analyzed using FACS Express software (version 3.06; De Novo Software, Glendale, CA, USA). The distribution of the individual cell population in the G1 (quiescent), S, and G2 (proliferative) phases of the cell cycle was determined.

Western blot analysis

The Western blot assay was performed according to an optimized and published protocol.⁸ The cells were treated with VY at concentrations of 40 and 80 µg/mL. Cells without any treatment served as the control. An equal quantity of cellular proteins was separated on 10% sodium dodecyl sulfate—polyacrylamide gels (SDS-PAGE; Mini-PROTEAN TGX, Bio-Rad Laboratories). The gels were directly incubated with relevant primary and secondary antibodies (see Supplementary Table).

The chemiluminescent signal was developed with ECL-plus reagent (Bio-Rad Laboratories) and detected by autoradiography. The signal intensity of β -actin (loading control) was used to normalize the signal intensity of cellular proteins. The signal intensity of proteins was quantified using a Molecular Imager GS800 and Quantity One software (Bio-Rad Laboratories) and was presented as arbitrary scanning units. Additionally, these data are presented as the total protein: β -actin ratio.

Cellular apoptosis assay

The presence of cells in the sub-G0/G1 (apoptotic) phase of the cell cycle was monitored by flow cytometry. Cells treated with VY at concentrations of 20, 40, and 80 µg/mL and the untreated control were sorted, and the apoptotic cell population was determined. The data are presented as the percentage of sub-G0/G1 cells.

Caspase 3/7 assay

An optimized, published protocol⁸ for caspase 3/7 activity used the Caspase-Glo assay kit (Promega Corporation, Madison, WI, USA). A cellular homogenate prepared from the cells treated with VY at 20, 40, and 80 μ g/mL and a homogenate from untreated cells were used to measure caspase 3/7 activity. The luminescence was measured using a luminometer (Thermo Fisher Scientific Inc,

Waltham, MA, USA). The data were expressed as RLUs.

Effect of pan-caspase inhibitor

To examine the functional specificity of caspase activity, the synthetic peptide pan-caspase inhibitor Z-VAD-FMK (Cell Signaling Technology; catalog No. 60332) was used. The untreated control, cells treated with 80 μ g/mL of VY, cells treated with 10 μ M of Z-VAD-FMK, and cells treated with VY + Z-VAD-FMK were processed for the measurement of caspase 3/7 activity. The data were presented as RLUs.

Statistical analysis

The experiments for dose response, caspase activity, and pan-caspase inhibitor were conducted in triplicate, and data are presented as mean (SD). The experiments for cell cycle progression and RB signaling were conducted in duplicate, and the data are presented as arithmetic means. Dunnett multiple comparison test was used as a post hoc test of 1-way analysis of variance (ANOVA). Moreover, an independent sample Student t test was used for comparison between multiple treatment groups and a common control group. Data analysis was carried out using Microsoft Excel 2013 XLSTAT-Base software. The generated P values are reported. P < 0.05 was considered to indicate a statistically significant difference.

RESULTS

Dose response of VY

This experiment was conducted to determine the range of growth inhibitory concentrations in response to treatment with VY. The growth of MDA-MB-231 cells was inhibited in a dose dependent manner as evidenced by reductions in cell viability. VY concentrations of 20, 40, 80, 100 and 400 μ g/ml exhibited inhibition rates of 53.8%, 61.3%, 76.9%, 84.6% and 92.3%, respectively, relative to the untreated control (Table 1). This dose response identified 18.6 μ g/ml of VY as the 50% inhibitory concentration.

Effect of VY on anchorage independent (AI) colony formation

This experiment was conducted to examine the effect of VY on the formation of AI colonies. AI colony formation represents an in vitro surrogate endpoint for tumorigenic cells. The data presented demonstrates that in response to treatment with VY at the concentrations of 100, 500 and 1,000 μ g/ml the AI colony number was found to decrease the inhibition rates by 42.9%, 63.7% and 91.9% respectively, relative to untreated control (Table 2).



Table 1. Growth-Inhibitory Dose Response of *Viola yedoensis*

Treatment	Concentration,	Relative luminescent unit,	P value	Inhibition,
	μg/mL	mean (SD)		% of control
Control	_	1.3 (0.3)	_	_
VY	20	0.6 (0.3)	0.04	53.8
	40	0.5 (0.3)	0.04	61.5
	80	0.3 (0.1)	0.02	76.9
	100	0.2 (0.1)	0.01	84.6
	400	0.1 (0.05)	0.01	92.3

VY, Viola yedoensis. Data were analyzed by analysis of variance with Dunnett multiple comparison test ($\alpha = 0.05$). The 50% inhibitory concentration for VY was 18.6 μ g/mL. N=3 per treatment group.

These data on AI colony formation identified $196.5~\mu g/mL$ of VY as the 50% inhibitory concentration.

Effect of VY on cell cycle progression

The data generated from this experiment demonstrated that VY treatment resulted in arrest of cells at the S phase of cell cycle in a dose-dependent manner. The G2 phase of the cell cycle was found to be progressively decreased and was undetectable in response to the maximum cytostatic concentration of $80 \mu g/ml$ VY. Control versus VY $80 \mu g/mL$: % S P=0.01. G2 phase: Not detectable.

The VY treatment groups were compared with a common control group. The P values for VY at 20 μ g/mL were as follows: % S, P = 0.5; % G2, P = 0.5. The P values for VY at 40 μ g/mL were as follows: % S, P = 0.04; % G2, P = 0.04 (Figure 1A).

Representative DNA histograms documented the effects of VY on cell cycle progression. Similar to the data in Figure 1A, DNA histograms demonstrated a progressive decrease in the G2 phase of the cell cycle and abrogation of the G2 phase in response to treatment with the higher dose of VY (Figure 1B–E).

Table 2. Growth inhibitory dose response of *Viola yedoensis*

Treatment	Concentration (µg/mL)	Relative Luminescent Unit (RLU)	P	Inhibition (% Control)
Control		1.3±0.3		
VY	20	0.6 ± 0.3	0.04	53.8
	40	0.5 ± 0.3	0.04	61.5
	80	0.3 ± 0.1	0.02	76.9
	100	0.2 ± 0.1	0.01	84.6
	400	0.1 ± 0.05	0.01	92.3

Data presented as mean \pm SD, N=3 per treatment group and analyzed by analysis of variance with Dunnett's Multiple Comparison Test (α =0.05). VY IC50: 18.6 μ g/ml. VY, Viola yedoensis.

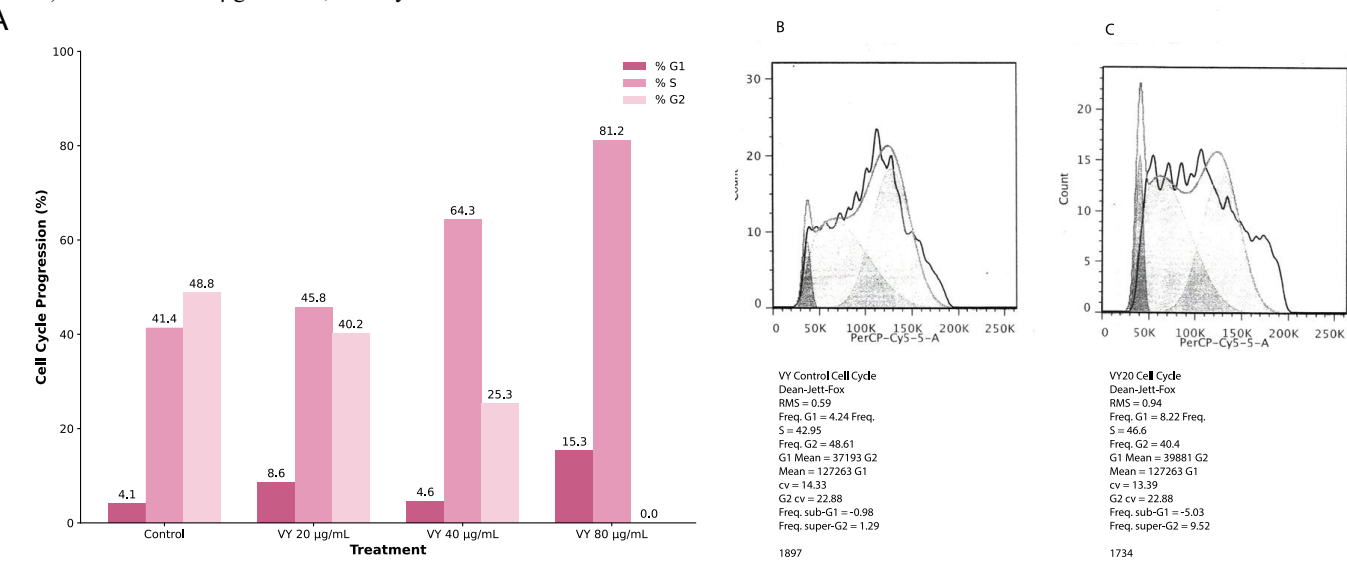


Figure 1. Effect of *Viola yedoensis* (VY) on Cell Cycle Progression. A, VY treatment resulted in the arrest of cells in the S phase of the cell cycle and abrogation of the G2 phase of the cell cycle at a higher concentration of VY. Data are presented as arithmetic means from 2 independent experiments. Control vs VY 80 μ g/mL: % S, P = 0.01; G2 not detectable. B–E, Representative DNA histograms for control and VY-treated cells. B, Control: S, 42.9%; G2, 48.6%. C, VY 20 μ g/mL: S, 46.6%; G2, 40.4%. D, VY 40 μ g/mL: S, 63.6%; G2, 25.7%. E, VY 80 μ g/mL: S, 81.2%; G2, 0%.

Effect of VY on retinoblastoma signaling

The RB signaling pathway operates during the G1–S phase and/or S–G2 phase transition of cells. For the S–G2 phase transition, the expression status of cyclin E (encoded by CCNE1), CDK2 (CDK2), pRB (RB1), and E2F1 (E2F1) is critical. The data demonstrated that VY at a concentration of 80 μ g/mL inhibited the expression of cyclin E, CDK2, pRB, and E2F1, relative to the untreated control (Figure 2A).

The data presented as the total protein: β -actin (ACTB) ratio demonstrated that in response to treatment with 80 µg/mL of VY, cyclin E expression decreased by approximately 78% (P=0.02), CDK2 expression decreased by approximately 47% (P=0.04), pRB expression decreased by approximately 31% (P=0.04), and E2F1 expression

decreased by approximately 92.3% (P = 0.01), relative to the control (Figure 2B).

Treatment with VY at 40 μ g/mL did not significantly affect the expression of cyclin E (P=0.5), CDK2 (P=0.5), pRB (P=0.5), or E2F1 (P=0.5), relative to the control.

Effect of VY on cellular apoptosis

The experiment designed to examine the effect of VY on cellular apoptosis monitored the population of cells in the sub-G0 phase of the cell cycle. The data demonstrated that VY treatment resulted in a dose-dependent increase in the cell population in the sub-G0 phase of the cell cycle. Treatment with VY at a concentration of $80 \mu g/mL$ induced an approximately 9.8-fold increase (P = 0.01) relative to the untreated control (Figure 3A).

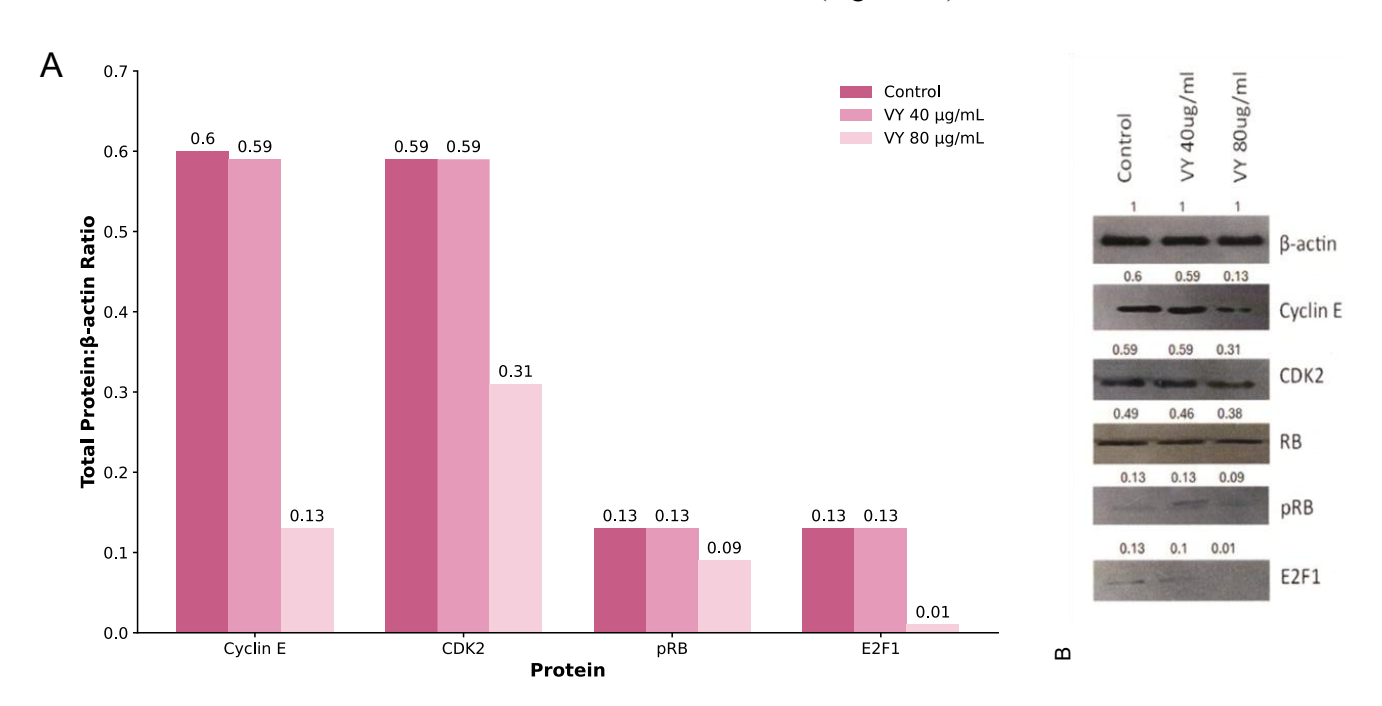


Figure 2. Effect of VY on Retinoblastoma (RB) Signaling. A, Representative Western blot assay shows a concentration-dependent inhibition of cyclin E, CDK2, phosphorylated RB (pRB), and E2F1 expression after treatment with VY. B, Data are presented as the total protein to β-actin ratio. Arithmetic means from 2 independent experiments are shown. Statistical significance was determined for control vs VY 80 μg/mL: cyclin E (P = 0.02), CDK2 (P = 0.04), pRB (P = 0.04), and E2F1 (P = 0.01).

At the mechanistic level, VY treatment resulted in a dose-dependent increase in caspase 3/7 activity. VY at a concentration of 80 μ g/mL induced an 18.8-fold increase (P = 0.01) in caspase 3/7 activity relative to the untreated control (Figure 3B).

The experiment designed to confirm the functional specificity of caspase 3/7 induction used the pancaspase inhibitor Z-VAD-FMK. The data presented

in Figure 3C demonstrated that VY at a concentration of 80 μ g/mL increased caspase 3/7 activity by approximately 8.8-fold (P=0.01) relative to the untreated control, and the VY-induced caspase activity was inhibited by approximately 57.1% (P=0.04) in response to treatment with Z-VAD-FMK relative to treatment with VY alone (Figure 3C).

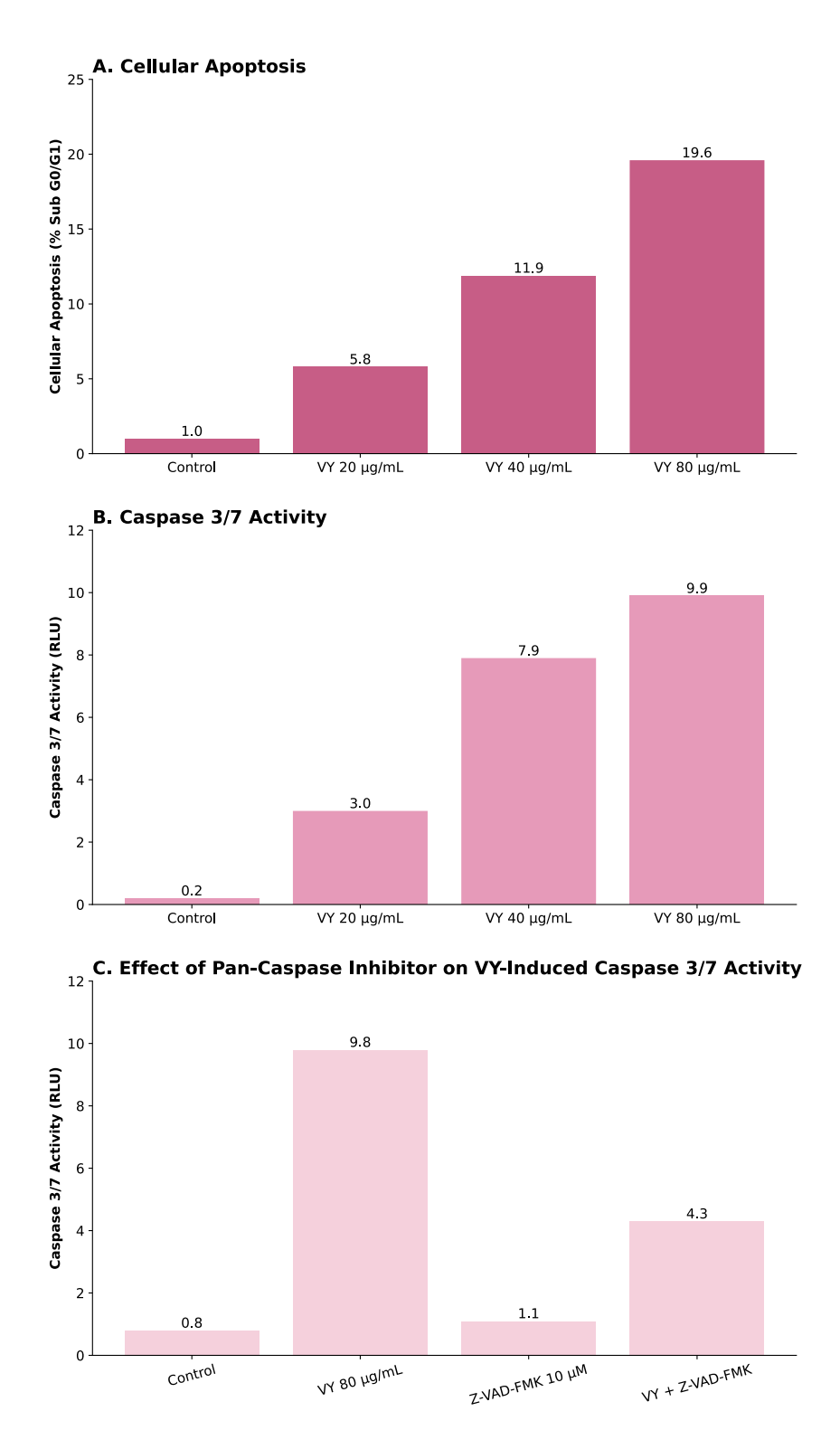


Figure 3. A: Effect of VY on cellular apoptosis VY treatment exhibited a concentration-dependent increase of cells in Sub G0 (apoptotic) phase of the cell cycle. Data are presented as mean \pm SD, N=3 per treatment group. Control versus VY 80 µg/mL, P=0.01. B: Effect of VY on caspase 3/7 activity. VY treatment induced a concentration-dependent increase in caspase 3/7 activity. Data are presented as mean \pm SD, N=3 per treatment group. Control versus VY 80 µg/mL, P=0.01. C: Effect of pan caspase inhibitor Z-VAD-FMK on VY-induced increase in caspase 3/7 activity. Control versus VY 80 µg/mL, P=0.01. Combination of VY+Z-VAD-FMK decreased caspase 3/7 activity. VY versus VY+Z-VAD-FMK P=0.04.

DISCUSSION

The American Cancer Society has estimated that there will be 310 726 new cases of breast cancer and 42 250 breast cancer–related deaths in 2025. 15 Breast cancer subtypes such as luminal A, luminal B, and HER2-enriched that express hormone and/or growth factor receptors exhibit a favorable response to endocrine and/or HER2-targeted therapies. contrast, the TNBC subtype lacks the expression of the estrogen receptor α (*ESR1*), progesterone receptor (PGR), and human epidermal growth factor receptor 2 (ERBB2). The TNBC subtype is noted to readily acquire resistance to a range of long-term conventional cytotoxic chemotherapies, such as anthracyclines (including doxorubicin), platinum agents (such as carboplatin), and taxanes (such as paclitaxel). The TNBC subtype has also been known to harbor a therapy-resistant, cancer-initiating stem cell population, which proliferates following chemotherapy.^{2,16} The TNBC subtype is notable for tumor heterogeneity, predominantly due to extensive cellular plasticity and phenotypic diversity. Among the multiple subtypes of TNBC, the mesenchymal (M) TNBC subtype shows the presence of putative stem cells. The MDA-MB-231 cell line model for TNBC belongs to the M TNBC subtype. 16

Experiments in the present study were designed on the MDA-MB-231 model to examine the growthinhibitory effects of VY. This nutritional herb contains multiple bioactive agents, including polyphenols, flavones, terpenes, saponins, and coumarins. 10,17 It is therefore conceivable that these agents, either individually or in combination, may influence the growth of MDA-MB-231 cells. The data generated using the nonfractionated aqueous extract of VY provide a basis to conduct specific bioactivity-guided experiments focused on fractionation of the VY extract. Chromatographic separation of individual fractions and chromatography-mass spectrometry-based detection of individual bioactive agents in each fraction may confirm their biological activity, mechanism(s) of action, and identify potential molecular targets. Collectively, these experiments may provide evidence for the growth-modulatory effects of individual bioactive fractions.

The growth-inhibitory effects of VY on triplenegative MDA-MB-231 cells were evidenced as a reduction of cell viability in adherent 2-dimensional cultures, as well as in the number of AI colonies formed in nonadherent 3-dimensional cultures. AI colony formation represents an in vitro surrogate marker for in vivo tumor formation. Collectively, these data provide evidence for VY-mediated susceptibility for growth inhibition, suggesting a possible reduction of breast cancer risk.

The RB signaling pathway represents one of the major tumor suppressor pathways responsible for the regulation of cellular proliferation and apoptosis. The tumor-suppressive function of RB is frequently compromised in clinical TNBC.^{3,4} In the MDA-MB-231 model for TNBC, defective RB signaling is associated with accelerated cell cycle progression due to the inactivation of negative growth-regulatory proteins and inhibition of cellular apoptosis. ¹⁸ The RB signaling pathway targets the G1-S phase transition via the cyclin D1 (CCND1)-CDK4 (CDK4)-CDK6 (CDK6)-pRB (RB1)-E2F1 (E2F1) axis and the S-G2/M phase transition via the cyclin E (CCNE1)-CDK2 (CDK2)-pRB (RBI)-E2F1 (E2FI) axis. In the RB signaling cascade, the expression of the E2F family of transcription factors represents a critical event preceding the expression of RB target genes. 19,20 In the present study, VY at the maximum cytostatic dose of 80 µg/mL downregulated the expression of cyclin E, CDK2, pRB, and E2F1.

The growth-inhibitory efficacy of the nutritional herbs CO, DA, and PC in the present TNBC model is associated with the inhibition of RB signaling through the cyclin D1-CDK4/6-pRB axis.^{5,6} Additionally, treatment with DA results in the inhibition of RAS (RAS), PI3K (PIK3CA), and AKT (AKT1), all of constitutively which activated are cancer cells.8,10,21,22 hyperproliferative Growth inhibition by Drynaria fortunei is effective via the inhibition of cyclin E, CDK2, pRB, and E2F1 expression. In the present study, treatment with VY resulted in the inhibition of cyclin E, CDK2, pRB, and E2F1. Collectively, these data suggest that individual nutritional herbs may affect the expression of distinct regulatory proteins involved in the RB signaling pathway.

In the present study, treatment with VY resulted in the induction of caspase 3/7 activity that was inhibited in the presence of the pan-caspase inhibitor Z-VAD-FMK. These data provide evidence for the functional significance of proapoptotic caspases, suggesting that VY may affect additional apoptosis-related markers.

The experimental approach using the present TNBC model provides several scientifically robust rationales for future investigations. Reliable cancer cell models may represent experimental approaches for examining the cancer stem cell-targeting efficacy of naturally occurring bioactive agents present in nutritional herbs.²³ Cancer stem cell-specific telomerase activity,²⁴ epigenetic modulation,²⁵ and stem cell plasticity through epithelial-mesenchymal transition²⁶ represent some approaches to identify additional therapeutic targets. Naturally occurring bioactive agents present in dietary phytochemicals and nutritional herbs that



target these processes^{27,28} may also represent novel drug candidates for therapy-resistant breast cancer.

CONCLUSION

These data identify the growth-inhibitory mechanism of VY, thereby providing a validated experimental approach to identify nutritional herbs as potential therapeutic alternatives for breast cancer.

ACKNOWLEDGMENTS

This study is dedicated to the memory of the late George Y-C. Wong, PhD. Dr Wong inspired and initiated research projects on the preventive efficacy of Chinese nutritional herbs on breast cancer. His conceptual and technical expertise in translating the clinical aspects of herbal medicine into mechanism-based evidence for preclinical efficacy have defined a scientifically robust rationale for current and future research directions.

FUNDING

Major support for the present research was provided by a philanthropic contribution from the Sophie Stenbeck Family Foundation to the American Foundation for Chinese Medicine. This research has not received any extramural funding from any governmental granting agencies.

REFERENCES

- 1. Lin NU, Vanderplas A, Hughes ME, Theriaukt RL, Edige SB, et al. Clinico-pathological features, patterns of recurrence and survival among women with triple-negative breast cancer in the National Comprehensive Cancer network. *Cancer* 2012, 118, 5463-5472, doi: 10.1002/cncr.27581.
- 2. Gradishar WJ, Moran MS, and Abraham J: Clinical practice guidelines in oncology: Breast cancer version 4, 2022.
- 3. Velloso FJ, Bianco FJR, Farias JO, Torres NEC, Ferruzo PYM, et al. The crossroads of breast cancer progression: Insights into the modulation of major signaling pathways. *Onco Targets and Therapy* 2017, 10: 5491-5524. doi: 10.2147/OTT.s142154.
- 4. Won KI and Spruck C: Triple-negative breast cancer therapy: Current and future perspectives. *Int J Oncol*. 2020, 57: 1245-1261. doi: 10.3892/ijo.2020.5135.
- 5. Telang NT, Nair HB, Wong GYC. Growth inhibitory efficacy of *Cornus officinalis* in a cell culture model for triple-negative breast cancer. *Oncol Lett.* 2019, 17: 5261-5266. doi: 10.3892/ol.2019.10182.
- 6. Telang NT, Nair HB, Wong GYC. Growth inhibitory efficacy of the nutritional herb *Psoralia corylifolia* in a model for triple-negative breast cancer. *Int J Funct Nutr.* 2021, 2: 8. doi: 10.3892/ijfn.2021.18.
- 7. Telang NT, Nair HB, Wong GYC. Growth inhibitory efficacy of Chinese herbs in a model for triple-negative

CONFLICT OF INTEREST

The authors declare no conflict of interest.

ETHICAL CONSIDERATIONS

Ethics approval and consent to participate are not applicable. This study did not use any clinical samples or require patient accrual.

DATA AVAILABILITY

The data presented in this manuscript, data analyses, and relevant materials will be made freely available upon reasonable request to the corresponding author.

AI DISCLOSURE

No AI tools were used in the preparation of this manuscript.

AUTHOR CONTRIBUTIONS

NTT: Conceptualization, Writing – Original Draft, Writing – Review & Editing. HBN: Project Administration, Investigation. GYCW: Data Curation, Formal Analysis, Funding Acquisition, Project Administration, Writing – Original Draft, Writing – Review & Editing.

- breast cancer. *Pharmaceuticals (Basel)* 2021, 14: 1318. doi: 10.3390/ph14121318.
- 8. Telang N, Nair HB, Wong GYC. Anti-proliferative and pro-apoptotic effects of *Dipsacus asperoides* in a cellular model for triple-negative breast cancer. *Arch Breast Cancer* 2022, 9: 66-75. doi: 10.32768/abc.20229166-75.
- 9. Telang N, Nair HB, Wong GYC. Anti-proliferative effects of *Drynaria fortunei*, in a cellular model for triple-negative breast cancer. *Oncol Letts*. 2025, 29: 91. doi: 10.3892/ol.2024.14837.
- 10. Yang Z, Zhang Q, Yu L, Zhu J, Cao Y, et al. The signaling pathways and targets of traditional Chinese medicine and natural medicine in triple-negative breast cancer. *J Ethno-Pharmacol*. 2021, 264: 113249. doi: 10.1016/jep.2020.113249.
- 11. Rizwan K, Khan SA, Ahmad I, Rasoool N, Ibrahim M, et al. A comprehensive review on chemical and pharmacological potential of *Viola betonicifolia*: A plant with multiple benefits. *Molecules* 2019, 24: 3138
- 12. Jeong YH, Oh YC, Cho WK, Shin H, Li KY, et al. Anti-inflammatory effects of *Viola Yedoensis* and the application of cell extraction methods for investigating bioactive constituent in macrophages. *BMC-Comp Alt Med.* 2016, 16:180.
- 13. Huang SF, Chu SC, Hsieh YH, Chen PN, Hsieh YS. Viola yedoensis suppresses cell invasion by targeting

- the protease and NF-kB activities in A549 and Lewis lung carcinoma cells. *Int J Mol Sci.* 2018, 15: 280-290.
- 14. Neeve RN, Chin K, Fridlyand J, Yeh J, Baehner FL, et al. A collection of breast cancer cell lines for the study of functionally distinct cancer subtypes. *Cancer Cell* 2006, 10: 515-527. doi: 10.1016/j.ccr.2006.10.008.
- American Cancer Society: Cancer Facts & Figures 2024. Atlanta, GA. American Cancer Society, 2024. https://www.cancer.org/content/dam/cancerorg/research/cancer-facts-and-figures/stasitics/annualcancer-facts-and-figures/2024/2024-cancer-facts-andfigures.pdf. (Assessed on May 10, 2025).
- 16. Lehmann BD, Colaprico A, Silva TC, Chen J, Hanbing A, et al. Multi-omics analysis identifies therapeutic vulnerabilities in triple-negative breast cancer subtypes. *Nat Commun.* 2021, 12: 6276.
- 17. Nagaprashantha LD, Adhikari R, Singhal J, Chikara S, Awasthi S, et al. Translational opportunities for broad spectrum natural phytochemicals and targeted agent combinations in breast cancer. *Int J Cancer* 2018, 142: 658-670. doi: 10.1002/ijc.31085.
- 18. Burkhart DL, Sage J. Cellular mechanisms of tumor suppression by the retinoblastoma gene. *Nat Rev Cancer* 2008, 8: 671-682. doi: 10.1038/nrc.2399.
- 19. Chen H-Z, Tsai S-Y, Leone G. Emerging roles of E2Fs in cancer: An exit from cell cycle. *Control Nat Rev Cancer* 2009, 9: 785-797. doi: 10.1038/nrc.2696.
- 20. Otto T, Sicinski P. Cell cycle proteins as promising targets in cancer therapy. *Nat Rev Cancer* 2017, 17: 93-115. doi: 10.1038/nrc. 2016.138.

- 21. Nussinov R, Tasi CJ, Jang H. Oncogenic Ras isoforms signaling specificity at the membrane. *Cancer Res.* 2018, 78: 593-602. doi: 10.1158/0008-5472.CAN-17-2727.
- 22. Costa RLB, Han HS, Gradishar WJ. Targeting the PI3K/AKT/mTOR pathway in triple-negative breast cancer: A review. *Breast Cancer Res Treat*. 2018, 169: 397-406. doi: 10.1007/s10549-018-4697-Y.
- Telang NT: Stem cell models for breast and colon cancer: Experimental approach for drug discovery. *Int* J Mol Sci. 2023, 23: 9223. doi: 10.3390/ijms 23169223.
- Hannen R, Bartsch JW. Essential roles of telomerase reverse transcriptase hTERT in cancer stemness and metastasis. *FEBS Letts*. 2018, 592: 2023-2031. doi: 10.1002/1873-3468.13084.
- 25. Kumar VE, Nambiar R, De Souza C, Nguyen A, Chien J, Lam KS. Targeting epigenetic modifiers of tumor plasticity and cancer stem cell behavior. *Cells* 2022, 11,1403.
- Gooding AJ and Scheiman WP: Epithelial-mesenchymal transition programs and cancer stem cell phenotypes mediators of breast cancer therapy resistance. *Mol Cancer Res.* 2020, 18: 1257-1270. doi: 10.1158/1541-7786MCR-20-0067.
- 27. Ganeshan K and Xu B: Telomerase inhibitors from natural products and their anti-cancer potential. *Int J Mol Sci.* 2017, 19: 13.
- 28. Liskova A, Kubatka P, Samee M, Zubar P, Mlynack M, et al. Dietary phytochemicals targeting cancer stem cells. *Molecules* 2019, 24: 899.

How to Cite This Article

Telang NT, Nair HB, Wong GYC. Growth Inhibitory Effects of a Chinese Nutritional Herb Viola yedoensis in a Model for Triple-Negative Breast Cancer. Arch Breast Cancer. 2025; 12(4):401-9.

Available from: https://www.archbreastcancer.com/index.php/abc/article/view/1132